Anat Embryol (1999) 200:103–115

ORIGINAL ARTICLE

Heidegard Hilbig · Hans-Jürgen Bidmon · Karl Zilles
Kirsten Busecke

Neuronal and glial structures of the superficial layers of the human superior colliculus

Accepted: 8 December 1998

Abstract We studied neuronal and glial elements in the superficial layers of the human superior colliculus by means of Nissl stains, Golgi impregnations, histochemical demonstration of NADPH-d activity and immunohistochemistry for glial fibrillary acidic protein (GFAP) in astrocytes. The glia-neuron interface was visualized with *Wisteria floribunda* agglutinin (WFA), which is a marker for perineuronal nets. The laminar pattern and the morphology of the major cell types closely resembled that found in other species although the thickness of the stratum zonale varied and the diversity of interneurons was greater than in other mammals. Furthermore, the stratum griseum superficiale showed a characteristic clustering of cells, the surfaces of which were intensely labeled by WFA. The clusters disappeared when GFAP expression increased.

Key words Glia-neuron interface · Golgi cell types · Lectin · GFAP · NADPH-d

Abbreviations *CG* Central grisea · *CGLd* corpus geniculatum laterale pars dorsalis · *DTN* dorsal terminal nucleus · *GFAP* glial fibrillary acidic protein · *NADPH-d* nicotinamide adenine dinucleotide phosphate diaphorase · *NHS* normal horse serum · *NOT* nucleus of the optic tract · *SC* superior colliculus · *SGS* stratum griseum superficiale · *SO* stratum opticum · *SZ* stratum zonale · *TBS* TRIS-buffered saline · *WFA Wisteria floribunda* agglutinin

H. Hilbig (✉) · K. Busecke
Institute of Anatomy, University of Leipzig, Liebigstrasse 13,
D-04103 Leipzig, Germany
Tel.: +49-341-97 22 053, Fax: +49-341-97 22 009

H.-J. Bidmon · K. Zilles
C. and O. Vogt Institute of Brain Research,
Department of Anatomy and Brain Research,
Heinrich Heine University, Moorenstrasse 5,
D-40225 Düsseldorf, Germany

Introduction

The SC is a mesencephalic structure involved in the control of eye movements. Eye movements have a high diagnostic value since they serve as important visible indicators of individual cognitive processes (Wurtz 1996). The diagnoses of eye movements are therefore important in an array of psychophysiological tests, yet the morphology and the mode of function of the human SC is still poorly understood (Laemle 1981, 1983). Most comparative studies have been done in other species. Functionally, the SC represents the mesencephalic relay station connecting cortex and brain stem. In rats, the SC receives most of its input directly from the cortex and area-specific visuo-cortical projections end in distinct regions (Harvey and Worthington 1990). In humans the deeper layers of the SC receive projections from the frontal and supplementary eye fields as well as the parietal cortex (Wurtz 1996). The upper layers receive cortical afferents from occipital areas. The upper layers are therefore thought to be directly involved in visually-guided eye movements. Furthermore, it has been suggested that the SC serves to integrate planed eye movements into the visual process (Robinson and McClurkin 1989).

In the upper layers of the rat SC it has been found that the proportion of projection neurons is about 70% (Hilbig 1996). In the CGLd about 93% are projection neurons (Werner and Krüger 1973) and the primary visual cortex contains 70–80% projection neurons (Werner et al. 1982). Thus the SC represents the region within the visual system with the proportionately largest number of interneurons in this species. Several histochemical studies have shown that the laminar organization of the SC can be functionally related to horizontally orientated sensory maps derived from physiological experiments.

Histochemical studies have in addition demonstrated that the SC has vertically oriented clusters of cells (Wallace 1986a,b; Illing 1988, 1989; Illing et al. 1990; Mize 1992). Cortical input to the upper layers of the SC seems to be diffusely distributed in mice and rats (Harvey and Worthington 1990; Hilbig 1991). By contrast, in visually

oriented species cortical terminals are segregated within the SC (cat: Harting et al. 1992). In what way this pattern of segregation may contribute to making visual functions more complex, remains to be explored. The ability to move the eye differs between rats and cats: only cats show eye movements. The functional and histological differences between the SC in other species are less obvious (Braun 1990; Davies 1991).

In the present study we investigated the cytoarchitecture of the superficial layers of the human SC. We compared the general cytoarchitectonic patterns in man to those that have been described in animal models. We also examined the Golgi cell types within the superficial layers. These layers are considered to be a relay station in the retino-tecto-pulvino-cortical pathway that probably represents a parallel path to the retino-geniculo-cortical one (Sugita et al. 1983; Huerta and Harting 1984).

The morphology of the cells in the upper layers has been described in detail for rats and mice (Tokunaga 1970; Valverde 1973; Langer and Lund 1974; Tokunaga and Otani 1976; Labriola and Laemle 1977). Most authors adhere to the system of Langer and Lund (1974) for classifying cell types in the SC and this system has been used to compare data on projection neurons in rats, hamsters, cats and tupaias (Graham and Casagrande 1980; Reese 1984; Mooney et al. 1985; Sahibzada et al. 1987).

Neurons positive for calcium binding proteins have been characterized within the human SC (Leuba and Saini 1996), but basic data on the packing density and layer-specific distribution of neurons and glial cells was up to now not available. The study of cell packing density is sometimes difficult in human brains since older subjects often show a varying degree of gliosis beneath the pia. We therefore also studied the distribution of astroglia by GFAP immunohistochemistry and of perineuronal nets (Celio and Blümcke 1994) that mark the glia-neuron interface or extracellular matrix. Components of this extracellular matrix such as proteoglycane seem to belong to region-specific properties. Proteoglycan components were detected using the N-acetylgalactosamine binding WFA. Additionally, WFA binding seems to depend on the function of the surrounded neuron (Kosaka and Heizmann 1989; Naegele and Katz 1990). Another marker for special types of neurons that was used in this study is neuronal NADPH-d, which is identical with nitric oxide synthase (Garthwaite 1995). NADPH-d active neurons are most likely to be interneurons, but large differences have been observed even in closely related species such as rat and hamster (Davies 1991).

Materials and methods

All procedures were approved by the ethical committee of the University of Leipzig.

For this study we used human autopsy brains of both sexes ranging in age from 56 to 81 (8–48 h post mortem). Either prior to or after fixation, the tissue was dissected from the whole brains such that each pair of colliculi remained together and were then sectioned transversely. Eight brains were fixed by immersion in 4% phosphate-buffered formalin (0.1 M PB, pH 7.4) for up to one year. Five SC were removed, dehydrated and embedded in paraffin. Serial 10-µm sections were stained according to Nissl (Romeis 1989). Three SC were removed, dehydrated and embedded in celloidin after having been treated en bloc with dichromate and silver nitrate according to Golgi-Bubenaite (Romeis 1989). These specimens were stored in 70% ethanol and sectioned at 150 µm.

Seven SC were used for GFAP and/or WFA labeling. The tissue was removed from the brains and fixed by immersion in Zamboni solution for several days. After cryoprotection by immersion in PB containing 15% sucrose for one day, followed by 30% sucrose in PB for two days, 10-µm-thick cryosections were prepared and mounted on glass slides.

NADPH-d histochemistry

Three SC were studied using the histochemical procedure for detection of NADPH-d activity after the protocol of Ellison et al. (1987). Free-floating sections were incubated in a solution containing 1 mM reduced β-NADPH and 0.8 mM nitroblue tetrazolium in 0.1 mM TRIS buffer (pH 8.0) at 37°C for 40–60 min. The reagents were obtained from Sigma. After incubation, the sections were rinsed in PB, air-dried and mounted with Entellan (Merck).

WFA

The sections were washed in 0.1 M TBS (pH 7.4) and endogenous peroxidase was blocked with 3% H_2O_2 for 30 min. They were then again rinsed in TBS and incubated in 3 µg biotinylated WFA (b-WFA, Sigma L-1766) per 1 ml TBS overnight at 4°C. After four rinses in TBS, they were incubated in AB complex (Vectastain) for 2 h and again rinsed in TB (50 mM, pH 7.6). The sections were then treated with DAB.

GFAP

The sections were washed in TBS (0.1 M) and endogenous peroxidase was blocked with 3% H_2O_2 for 30 min. After several rinses in TBS, they were incubated in 10% NHS in TBS for 30 min followed by 2% NHS in TBS containing antibodies to GFAP 1:40 (Boehringer, monoclonal G-A-5, mouse IgG1) and 0.1% Triton X-100 for 48 h at 4°C. After four rinses in TBS the sections were incubated in TBS containing 2% NHS and the second biotinylated anti-mouse antibody (Vectastain) at a final antibody dilution of 1:200 for 24 h at 4°C. Sections were then processed as for WFA.

WFA and GFAP fluorescence

After having incubated with biotinylated WFA as above, the binding sites were exposed with the fluorescent dye Cy2-conjugated streptavidin (Amersham) diluted 1:50 in TBS and applied for 4 h at room temperature. Following three rinses with TBS, sections for double labeling were placed in TBS with 1% BSA and a monoclonal antibody against GFAP labeled with Cy3 (Sigma, red fluorescence) at a dilution of 1:400 (4°C, 12 h). They were then rinsed three times with TBS, and coverslipped in Vectashield.

Control sections were treated with non-specific mouse antibodies (IgG1; DAKO) diluted and applied similarly to the specific antibodies.

Fig. 1A–C Nissl staining. **A** median part at intercollicular sulcus; *arrows* indicate differences in thickness of SZ. **B** Mid part of one colliculus; *arrowheads* indicate borders of laminae and sublaminae of SGS. *Asterisks* indicate cell-free parts. **C** Lateral part; *small arrowheads* mark end of SZ; *vertical arrowhead* marks border of SC. *Bars* 100 µm ▶

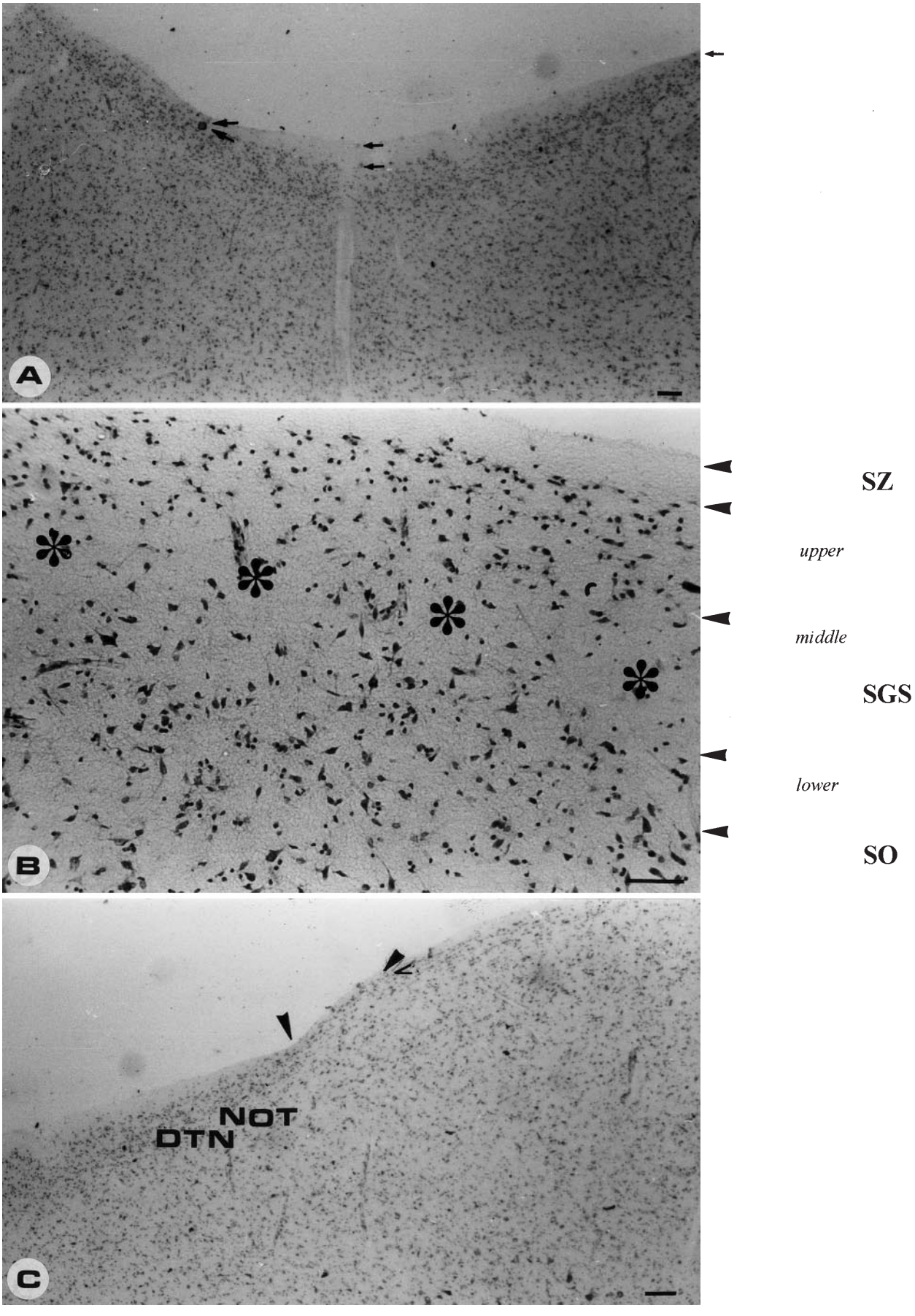
A
B
C
SZ
upper
middle
SGS
lower
SO
NOT
DTN

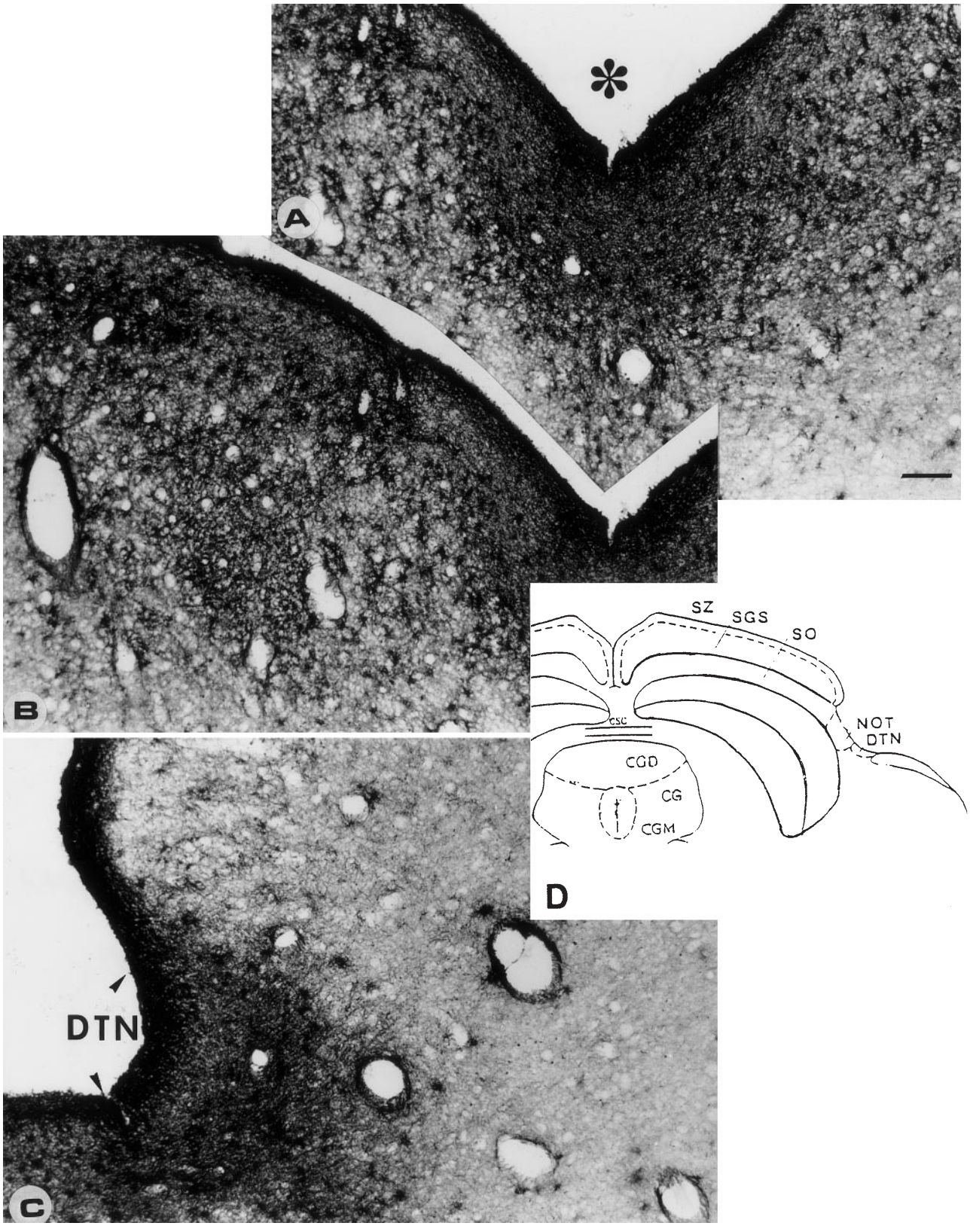

Fig. 2A–C WFA binding. **A, B** Median part at intercollicular sulcus; *asterisk* indicates the intercollicular sulcus. **C** Lateral part, comparable to Fig. 1C. Note that SZ is very densely labeled but that in other layers binding is rather patchy. *Bars* 100 µm. **D** Schematic drawings of the superior colliculus and its borders

Double-labeled sections were examined with a photomicroscope and in the LSM 410 confocal laser-scanning microscope (Zeiss, Germany) with excitation wavelengths at 488 and 568 nm.

Results

As in other mammals, the human SC can be divided into superficial and deep layers. Nissl-stained sections show a layering of the upper parts of the SC into the most superficial zone – the SZ, the ventrally adjacent SGS and the SO (Fig. 1). The SO continues into the deep layers without any sharp transition. The Nissl-stained sections showed that both neuronal and glial components were organized in strata-specific distribution patterns. Most of the SZ contained only few cells, especially in parts immediately beneath the pial surface. Regional differences were noted within the SZ: the fewest cells were seen at the medial and lateral borders of each colliculus. Small arrows in Fig. 1A indicate the nearly cell free medial part of the SZ, small arrows in Fig. 1C indicate the lateral part. The large arrow indicates the border of the SC and the NOT/DTN. Cells located close to the pial surface were found mainly between the extremes (Fig. 1B). The SZ gradually became thinner toward its lateral borders (arrows in Fig. 1C).

The SGS was easily delineated because both the number and variety of cell types were greater than in the SZ. The SGS could be divided into an upper, a middle and a lower sublamina on the basis of differences in cell packing density (Fig. 1B). The SGS within each colliculus also had a central region containing more cells than in median or lateral aspects (Fig. 1B). Most cells were small and had only narrow margins of cytoplasm. The sublaminae were separated by a thinner intermediate layer with fewer cells. This intermediate layer has cell-rich parts that alternate with spot-like cell-free parts (stars in Fig. 1B). The border of the SGS toward the SO is much less distinct than its border to the SZ. The SO possesses only a slightly lower cell packing density than the SGS. Similar to the other laminae, the SO becomes narrower laterally and is no longer detectable at the borders to the DTN and NOT.

In contrast to the Nissl-stained sections, those with WFA binding did not reveal any distinct lamination of the SC with the exception of the densely labeled SZ. Binding was most intense in subpial levels and gradually faded toward deeper levels without showing any major regional differences, although it was somewhat enhanced at the medial and lateral borders of the SC (Fig. 2A–C). Particularly intense binding was found in the depths of the intercollicular sulcus (Fig. 2A) and the deeper layers of the SC showed less binding laterally. Although there was no impressive Nissl-like lamination within the SC, WFA binding was inhomogeneous within the SGS. Patches of intense staining alternated with weakly labeled ones (Fig. 3). The strongly stained patches contained WFA-positive fibers and cells (Fig. 3B).

GFAP immunohistochemistry yielded patterns of labeling similar to those of WFA binding. The patchy distribution of binding seen in WFA sections, however, was not found in sections treated for GFAP. Figure 4 compares the amount of lipofuscin (white spots) and the labeling of GFAP positive structures during aging. Small gliosis on the pial surface or near the surface corresponded with small amounts of lipofuscin and the expression of GFAP in the astrocytes. But there were no strongly age-dependent alterations. Increased GFAP expression corresponded with decreased WFA binding. The patchy patterns were lost. Fig. 5 shows sections double-labeled for GFAP and WFA. Lipofuscin has white autofluorescence in UV light. It seemed that GFAP-positive gliosis masks or suppresses WFA binding sites at the glia-neuron

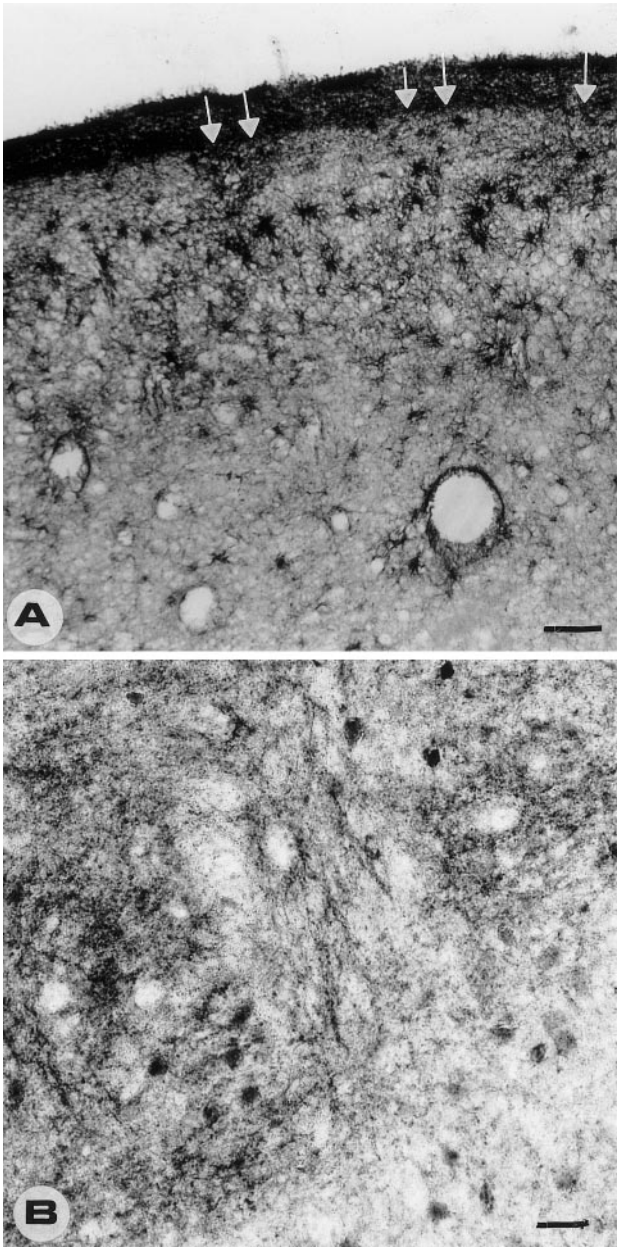

Fig. 3A, B WFA binding. **A** Homogeneous fibrous labeling in SZ; patchy binding in SGS (*arrows*). **B** Higher magnification of the borders of patches. *Bars* **A** 100 µm, for **B** 50 µm

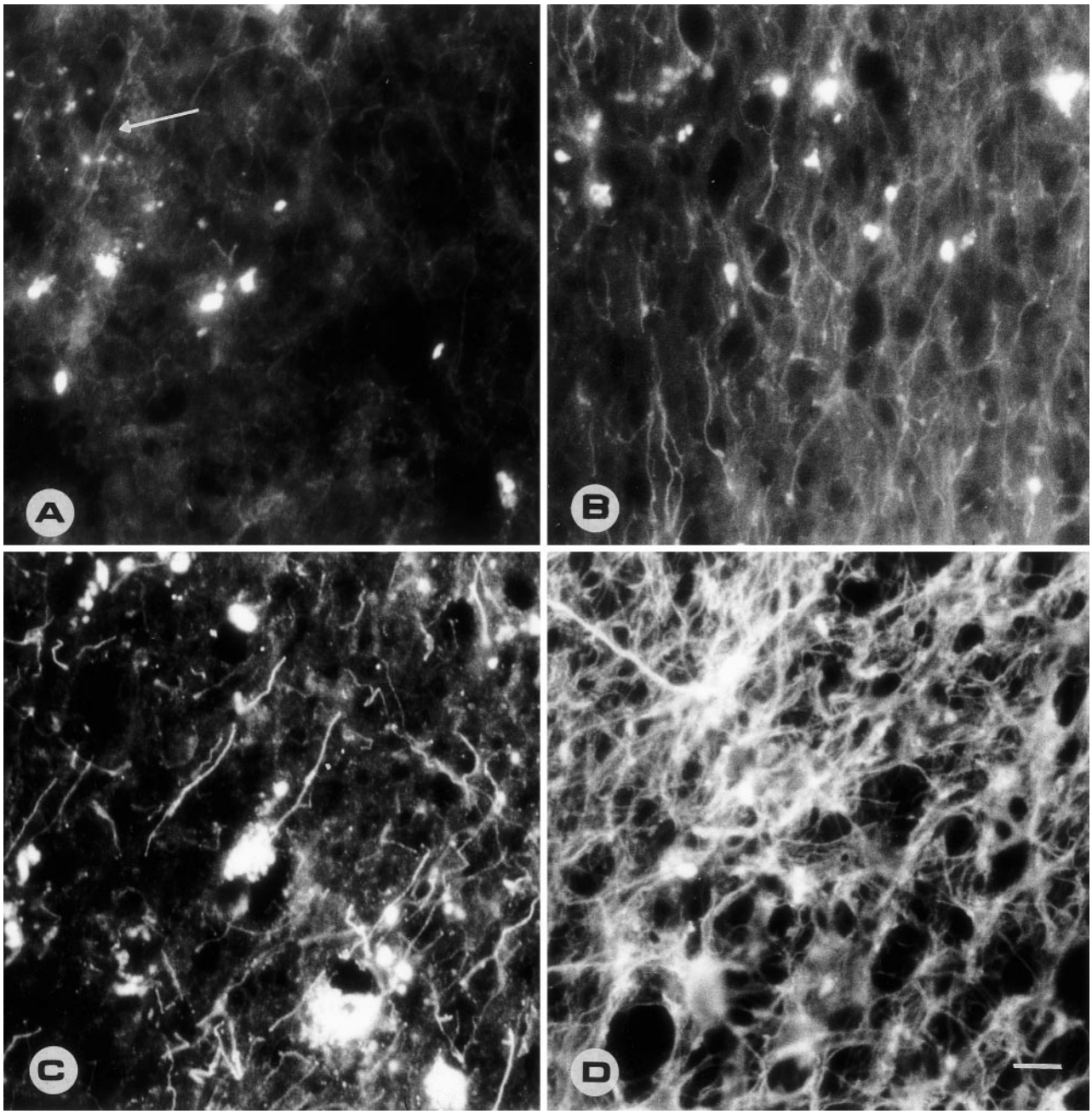

Fig. 4A–D GFAP expression and lipofuscin increase during aging. **A** Small expression of GFAP (*arrow*) corresponds with small amounts of lipofuscin (*spots*) at age 61 years. **B** 63 years. **C** 73 years. **D** 81 years. *Bar* 50 µm

interface (Fig. 5A, B). Whereas the GFAP-labeled (red) structures were clearly seen, structures with WFA binding seemed shadow-like. Only the walls of a large blood vessel contain clearly visible WFA-positive structures. (Fig. 5A). Here, the lipofuscin was widespread but distributed in small amounts. Figure 5B shows an overview of the SC with a higher content of lipofuscin and GFAP below the pia. WFA-labeling is nearly invisible (triangle in Fig. 5B). The complementary patterns of GFAP- and WFA-positive structures were demonstrated by the laser-scanning microscopy (Fig. 5C–E). Figure 5C shows the double-labeled blood vessel in a human SC at the age of 56 years. No lipofuscin was visible in the SC, gliosis was restricted to the pial surface and to the blood vessels. In the focus of Fig. 5C is a blood vessel with walls strongly labeled in green. Fig. 5D demonstrates GFAP-positive structures of the walls of the blood vessel and Fig. 5E shows it for WFA.

In summary, older human SC often contain lipofuscin and in that case WFA binding does not result in distinct patterns. The amount of WFA-positive material seems to be reduced; GFAP labeling is increased and was spread throughout the superficial layers of the SC.

The morphology of neurons showed no major differences to that of comparable neurons in other mammals.

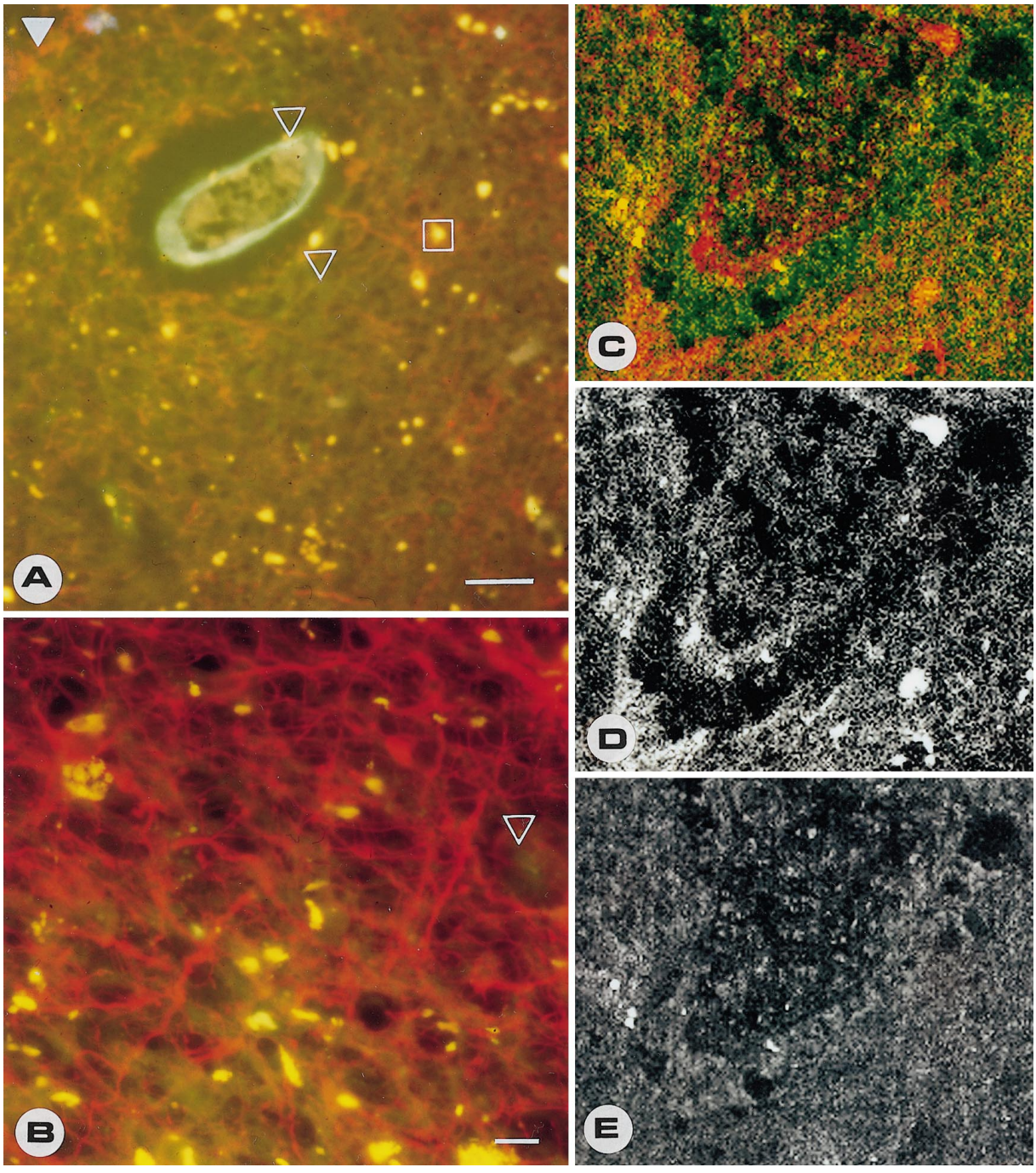

Fig. 5A–E Double treatment for GFAP (*red*) and WFA (*greenish*) demonstrates the complementary patterns of GFAP and WFA. Lipofuscin autofluorescence (*bright yellow*). **A** Clear GFAP positive structures, especially at the surface of the SC (*solid triangle*) and lipofuscin spots (*square*), shadow-like WFA structures (*open triangles*). *Bar* 100 µm. **B** Many GFAP-positive fibers but only very weak fluorescence for WFA (*open triangle*). *Bar* 50 µm, **C–E** Confocal laser-scanning micrographs of a brain blood vessel at ×2240. **D** documents GFAP only. **E** indicates WFA

Only in rare cases did the dendrites bear spines. Overviews of Golgi-impregnated sections showed lamination patterns comparable to those of Nissl sections. The lamination was indicated by the orientation of the dendritic fields: in SZ and in SO most of the neurons were horizontally oriented. In the SGS, the orientation of the cells was vertical (Figs. 6, 7).

The SZ contained neurons whose processes and small perikarya were oriented more or less parallel to the pial surface, even in median parts where the surface dips into the intercollicular sulcus (neurons 1–4 in Fig. 6). These cells have therefore been called horizontal cells. Some horizontal cells had dendrites that penetrated toward the SGS (1, 2, Fig. 6) and they have been classified by Langer and Lund (1974) as marginal cells.

The neurons in the three sublaminae of the SGS differed somewhat from one another, but many of them had

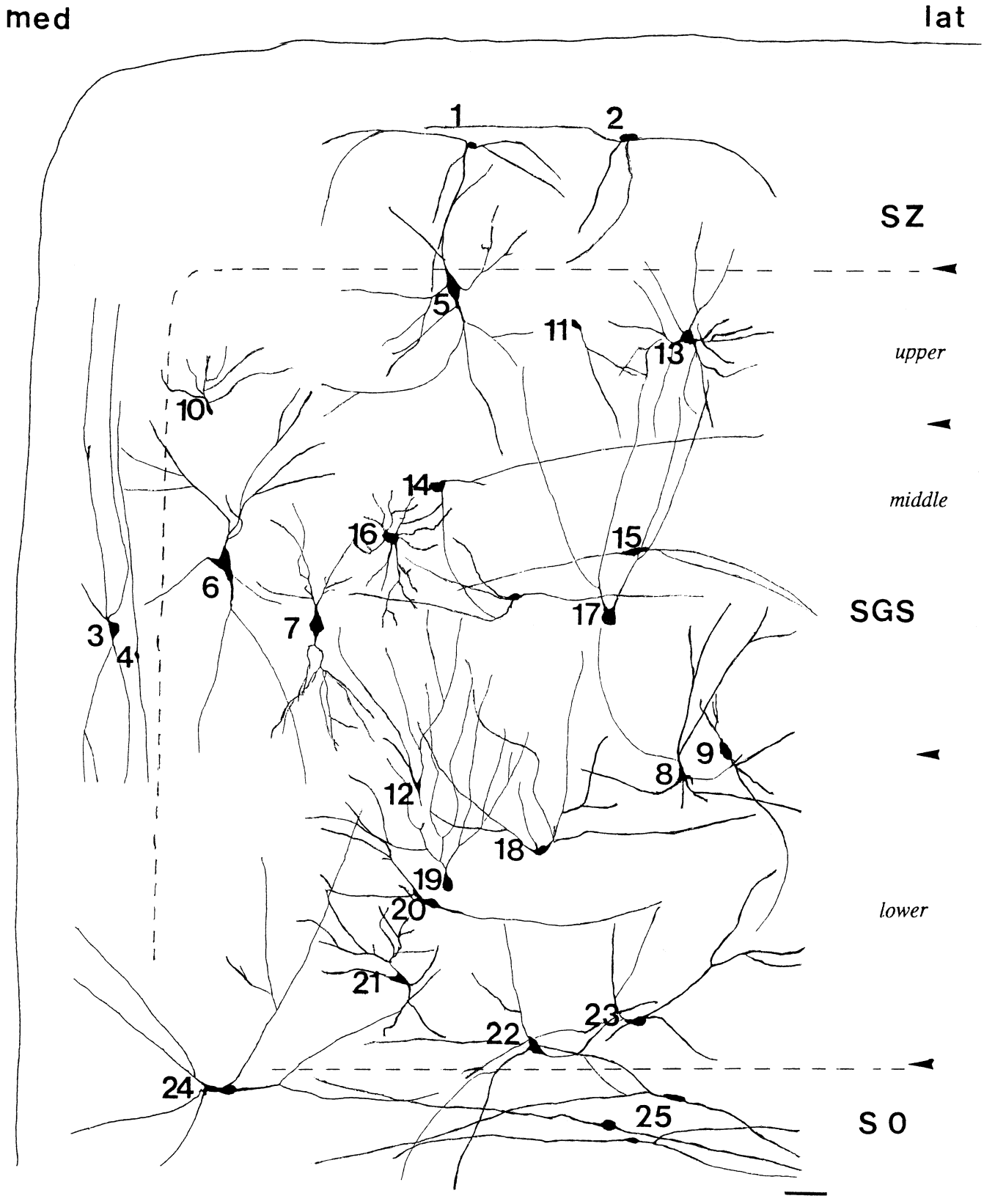

Fig. 6 Golgi morphology of neurons. For numbering see Results. *Bar* 20 µm

Fig. 7A–E Golgi-impregnated and NADPH-d positive neurons. **A, B** Vertically oriented neurons in the upper sublamina of SGS corresponding to neuron 5 of Fig. 6. **C** Horizontally oriented soma of a wide-field neuron in SO. **D** NADPH-d-positive marginal cells (neurons 1 and 2 of Fig. 6). **E** NADPH-d-positive cells of the mid SGS corresponding to neuronal type of neuron 6 (Fig. 6). The cell indicated by an *asterisk* represents a cell type not described until now for humans. *Bar* 50 µm ▶

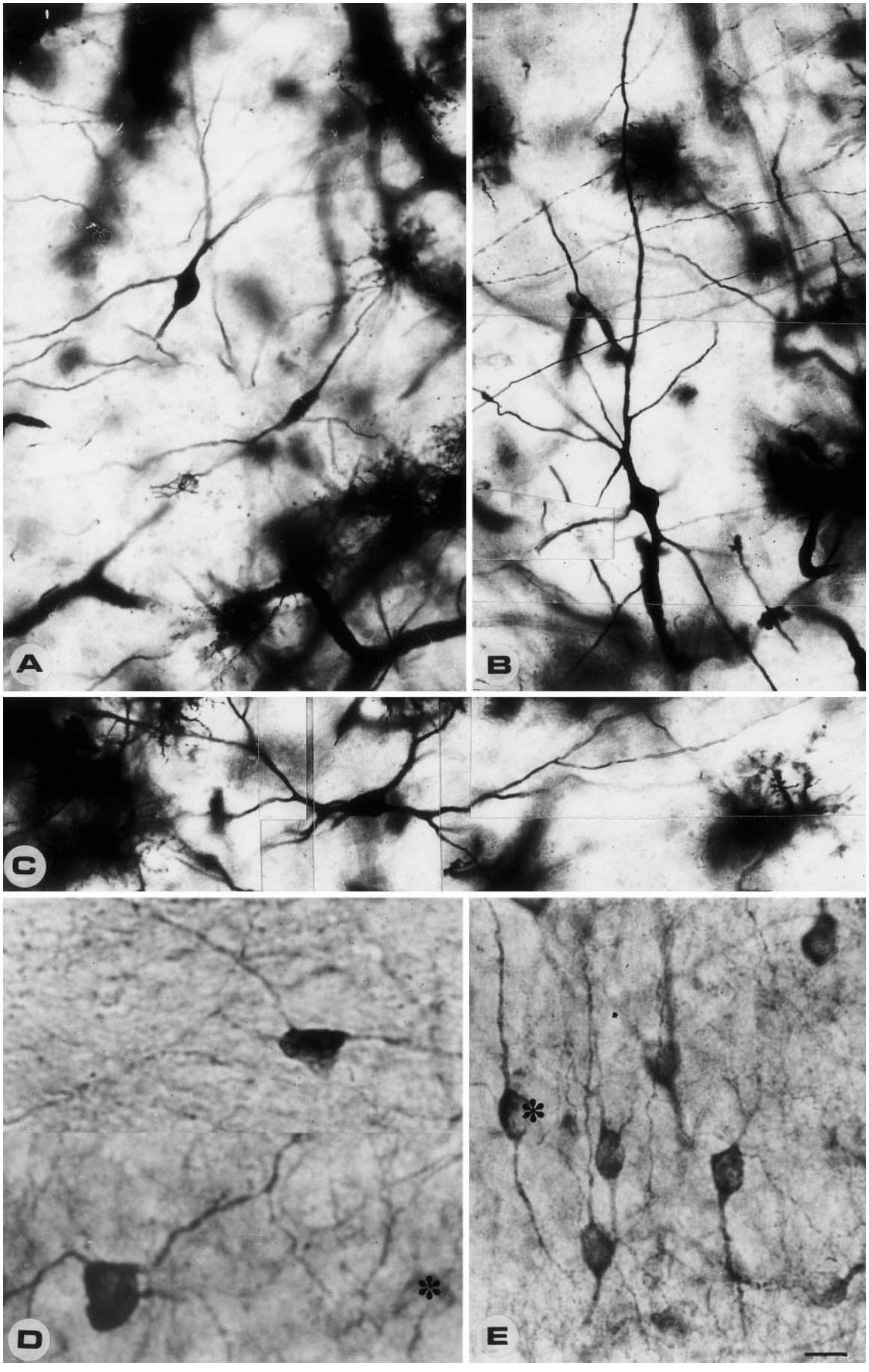
A
B
C
D
E

processes and perikarya which were oriented perpendicularly to the pial surface (Figs. 6, 7A,B). This orientation is readily evident in neurons 5–9 (Fig. 6). They had large- to medium-sized somata and poorly branched, almost spineless dendrites. The morphology of these neurons can be described as bi-tufted, since only few dendrites branched from the lateral parts of their somata. Some of those neurons were NADPH-d active (Fig. 7E). Scattered throughout the entire SGS one could find very small neurons of diverse shapes and orientations (10–12, Fig. 6). Only the upper sublamina had comparatively large neurons with fusiform somata and radially branching, spineless dendrites (13, Fig. 6). A few small neurons resembling horizontal cells were seen in the intermediate layer (14, 15, Fig. 6). Such cells were located at the edges or within relatively cell-free areas. Small, almost stellate neurons with spiny dendrites were located along the border between the intermediate and upper sublamina (16, Fig. 6). Neuron 17 in Fig. 6, which can be characterized as a piriform cell, was found in the middle of the intermediate layer. This type of neuron possesses only poorly branched dendrites oriented toward the pia. In the lower sublamina most neurons also had dendrites, oriented toward the surface. However, their somata and dendritic fields were small and highly variable (18–22, Fig. 6). These neurons cannot always be clearly distinguished from the so-called wide-field neurons (Langer and Lund 1974). Neuron 22 exhibits the horizontally oriented, medium-to large-sized soma and long, proximally spineless dendrites that are characteristic of wide-field cells. The dendritic fields may reach the upper sublamina. Wide-field neurons were present not only in the lowest regions of the SGS; they were also seen in the upper SO (23, 24, Figs. 6, 7C).

The SO contained horizontally oriented neurons of ovoid shape with long dendrites that did not leave the SO (25, Fig. 6). The neurons 1 and 2 revealed by Golgi staining showed an identical morphology with the NADPH-d active interneurons in Fig. 7D. Most of the neurons of the middle SGS were NADPH-d active too (Fig. 7E). The very small vertically oriented neuron indicated by a star represented a cell type not described, until now, for humans.

Summarizing, we found in the human SC neuronal structures resembling those of other vertebrates. The lamination pattern was not very impressive but was visible. The Golgi staining revealed all of the known cell types.

Glial structures of the human SC seemed to depend on gliosis that corresponded to the amount of lipofuscin and/or aging or other possible factors. During aging, the glial network of the SC changed from wide-spread WFA-positive structures to an increasing GFAP-network.

Discussion

Aspects of neuronal morphology

Most classifications of SC neurons follow the system introduced by Langer and Lund (1974). The vertically oriented medium-sized neurons in the upper sublamina of the SGS resemble small-field cells. They represent projection neurons to the CGLd (tupaia: Graham and Casagrande 1980; Grantyn 1988). The wide-field cells in the lower sublamina project to the lateral posterior nucleus of the thalamus (rat: Sugita et al. 1983). The cells we found at the border to the SO and within the SO may correspond to descending projection neurons seen in other species. The same holds true for neurons in the intermediate layer; similar ones are located in the rostro-medial part of the superficial layers of the SC in some animals (rat: Yamasaki et al. 1984; Hilbig and Schierwagen 1994; cat: Mize et al. 1991). The morphology and termination fields of projection neurons appear to be stereotypical and well-conserved among the various orders of mammals so far studied. However, small-field cells differ considerably with respect to the number of spines (Labriola and Laemle 1977). It is noteworthy that most human Golgi neurons have only a few spines. This condition may be due to post-mortal autolysis. Only Laemle (1981) described spines on certain types of dendrites within the human SC and these were generally located in superficial regions, suggesting that spines are lost in deeper regions, close to the perikarya, perhaps because the fixative does not penetrate rapidly enough. Many neurons within the human SC were interneurons and NADPH-d active. In rats comparable interneurons within the deep layers of the SC surrounded one or two much larger neurons (Gonzales-Hernandez et al. 1992; Hilbig and Winkelmann 1993). Such surroundings were not found in the human SC but there were the same patchings as in the rat. WFA-patches of the upper SGS of the superficial layers of the SC correspond with the NADPH-d active patches of neuropil in the intermediate layers of the SC (Busecke et al. 1996). The vertical columns are disrupted in the middle and lower SGS and in the SO. A continuously vertically oriented column could never be seen, either in rat or in man. It appears that the laminar arrangement of neurons within the superficial layers of the human SC is quite similar to that described for other mammals. Interestingly enough, cells similar to the horizontal cells (neurons 14 and 15, Fig. 6) located in the middle layer of the human SGS have not been described in other mammals, but have been seen in birds (Vanegas 1984). The horizontal cells with their relatively tiny somata and small dendritic fields are probably local interneurons. Their shapes are completely different from those of projecting neurons. Neurons of such small size are usually described as inhibitory neurons in humans (Leuba and Saini 1996).

Glia and the glia-neuron interface

Neuron-glia interactions are mediated by diverse cellular and molecular mechanisms, not only during morphogenesis but also during the modification of neural connectivity in the adult. Glial recognition molecules at the cell surface and in the extracellular matrix form boundaries depending on the functional state and nature of the neu-

ron (Pappas and Ransom 1994; Robello et al. 1994). One morphological equivalent to the normal physiological state in the human SC seems to be material positive for WFA- binding, whereas large quantities of GFAP may indicate a pathological alteration (gliosis).

Components of perineuronal nets (Celio and Blümcke 1994) such as GalNac 1–3, to which WFA lectin binds specifically, showed distribution patterns that in part resembled the patterns of lamination and cell packing density found in Nissl-stained sections. WFA binding may therefore be a useful tool for revealing functional, intralaminar subdivisions. However, in our tissue samples the pattern seen for WFA changed depending on gliosis (GFAP-labeling). It may be that only a subpopulation of astrocytes with specialized functions expressed binding sites for WFA. Brückner et al. (1994, 1996) and Seeger et al. (1994, 1996) were able to show that astrocytes are involved in maintaining the extracellular milieu of inhibitory cortical neurons via the WFA-labeled interface. Inhibitory neurons have been identified as essential elements in the processing of sensory information (Leuba and Saini 1996) and astrocytes contribute with glutamate uptake mechanisms, effective especially at synaptic clefts (Pellerin and Magistretti 1994). In the mouse cerebral cortex WFA binding appears late during development and is then intensely expressed in primary sensory areas as they become fully functional (Oermann 1996). Binding remains intense in these areas in adults (Brückner et al. 1994, Bidmon et al. 1997). WFA binding decreases rapidly (≤24 h) in areas in which synaptic integrity is lost, for example in the penumbra of ischemic lesions of the somatosensory cortex. It is noteworthy that massive astrocytosis and glial scar formation occur within a penumbra and around a lesion core, but WFA binding is not enhanced (Bidmon et al. 1998). This finding suggests that WFA expression is associated with functional integrity and signal transduction (Bertolotto et al. 1991; Brückner et al. 1994; Celio and Blümcke 1994). On the other hand WFA is only one component of the extracellular matrix and may be expressed by a subset of neurons (Lander et al. 1998). The regions immediately beneath the pia, which in most of our samples were intensely positive for both WFA and GFAP, may represent regions in which age-related pathological astrocytosis had occurred. They may also be indicative of pre-mortem or early post-mortem ischemic conditions that took place early enough to permit GFAP upregulation. It is well known that human brain tissue exhibits highly variable degrees of gliosis in association with the pia mater. If this general observation reflects the in vivo situation, or if it is a consequence of pre-mortem or early post-mortem conditions, remains to be clarified. The transformation of radial glia into astrocytes is a well-known phenomenon in both rodents (Publido-Caballero et al. 1994) and mammals (Levitt and Rakic 1980) and some of the astrocytes seen in human tissue may be derived from similar precursors. The major difference between the distribution patterns of WFA- and GFAP-positive elements was seen in the SGS. WFA-positive material appeared in patches whereas this did not hold true for GFAP-labeled structures. GFAP labeling was intense throughout the superficial layers of the SC. The middle layer of the SGS, also showed an inhomogeneous distribution of cells in the Nissl-stained sections. In animal models the upper sublamina corresponds to the region with the greatest input from the retina (Graham and Casagrande 1980; Grantyn 1988). The lower sublamina receives mostly cortical inputs (Hunt and Künzle 1976; Harvey and Worthington 1990). The patchy WFA-positive structures in the intermediate layer may participate in processes coordinating information from different sources. A patch-like distribution of axon terminals and enzyme activities has also been noted in the mid and lower SGS in animals (Graybiel et al. 1984; Illing and Graybiel 1993). Jeon and Mize (1993) described patches of acetylcholinesterase activity and NADPH-diaphorase in the SO and deeper regions of the cat SC. GFAP-positive astrocytes have been described in mammalian and submammalian vertebrates, which suggests that there are species-specific differences between the distribution patterns of GFAP-positive astroglia (Bignami and Dahl 1976; Lindsay 1986; Eng et al. 1987; Hajos and Kalman 1989; Zilles et al. 1991; Eddleston and Mucke 1993; Schmidt-Kastner et al. 1993; Eng and Ghirnikar 1994). On the other hand, aging is an individual process with wide variations. Especially in humans, it can depend on many factors. Recently, it was revealed (in rats) that decreasing levels of circulating steroid hormons may be responsible for the age-dependent gliosis in various brain regions and that the alterations can be partly corrected by the administration of pregnenolone (Legrand and Alonso 1998).

Conclusions

Neuronal structures of the human SC are arranged both as laminated and patched. Lamination was revealed by Nissl-staining and by distribution of Golgi-cell types. Patches were demonstrated by NADPH-d activity of the neuropil and by WFA-labeling of the glia-neuron interface. WFA does not seem to be related to the reactive state of glia, but may reflect certain functional glia-neuron interactions.

Acknowledgements The authors thank Dr. K. Rascher for discussions and Zeiss Germany for the support.

References

Bertolotto A, Rocca G, Canavese G, Migheli A, Schiffer D (1991) Chrondroitin sulfate proteoglycan surrounds a subset of human and rat CNS neurons. J Neurosci Res 29:225–234

Bidmon HJ, Wu J, Gödecke A, Schleicher A, Mayer B, Zilles K (1997) Nitric oxide synthase-expressing neurons are area-specifically distributed within the cerebral cortex of the rat. Neuroscience 81:321–330

Bidmon HJ, Jancsik V, Schleicher A, Hagemann G, Witte OW, Woodhams P, Zilles K (1998) Structural alterations and changes in cytoskeletal proteins and proteoglycans after focal cortical ischemia. Neuroscience 82:397–420

Bignami A, Dahl D (1976) The astroglial response to stabbing. Immunofluorescence studies with antibodies to astrocyte-spe-

cific protein (GFAP) in mammalian and submammalian vertebrates. Neuropathol Appl Neurobiol 2:99–110
Braun K (1990) Calcium-binding-proteins in avian and mammalian central nervous system: localization, development and possible functions. Fischer, Stuttgart New York
Brückner G, Seeger G, Brauer K, Härtig W, Kacza J, Bigl V (1994) Cortical areas are revealed by distribution patterns of proteoglycan components and parvalbumin in the Mongolian gerbil and rat. Brain Res 658:67–86
Brückner G, Brauer K, Härtig W, Kacza J, Seeger J, Welt K (1996) Extracellular matrix organization in various regions of rat brain grey matter. J Neurocytol 25:333–346
Busecke K, Hilbig H, Lüth HJ (1996) Untersuchungen zur Zellmorphologie des menschlichen Colliculus superior. Verh Anat Ges 91:200–201
Celio MR, Blümcke I (1994) Perineuronal nets – a specialized form of extracellular matrix in the adult nervous system. Brain Res Rev 19:128–145
Davies BJ (1991) NADPH-diaphorase activity in the olfactory bulb of the hamster and rat. J Comp Neurol 314:493–511
Eddlestone M, Mucke L (1993) Molecular profile of reactive astrocytes: implications for their role in neurological disease. Neuroscience 54:15–36
Ellison DW, Kowall NW, Martin JB (1987) Subset of neurons characterized by the presence of NADPH-diaphorase in human substantia innominata. J Comp Neurol 260:233–245
Eng LF, Ghirnikar RS (1994) GFAP and astrogliosis. Brain Pathol 4:229–237
Eng LF, Reier PJ, Houle D (1987) Astrocyte activation and fibrous gliosis: Glial fibrillary acidic protein immunostaining of astrocytes following intraspinal cord grafting of fetal CNS tissue. Prog Brain Res 71:439–455
Garthwaite J (1995) Neural nitric oxide signalling. Trends Neurosci 18:51–52
Gonzales-Hernandez T, Conde-Sendin M, Meyer G (1992) Laminar distribution and morphology of NADPH-diaphorase containing neurons in the superior colliculus and underlying periaqueductal gray matter of the rat. Anat Embryol 186:245–250
Graham J, Casagrande VA (1980) A light microscopic and electron microscopic study of the superficial layers of the superior colliculus of the tree shrew (*Tupaia glis*). J Comp Neurol 191:133–151
Grantyn R (1988) Gaze control through superior colliculus: structure and function. In: Büttner-Ennever B (ed) Neuroanatomy of the oculomotor system. Elsevier, Amsterdam, pp 273–333
Graybiel AM, Brecha N, Karten HJ (1984) Cluster-and-sheet pattern of enkephalin-like immunoreactivity in the superior colliculus of the cat. Neuroscience12:191–214
Hajos F, Kalman M (1989) Distribution of glial fibrillary acidic ptotein (GFAP)-immunoreactive astrocytes in the rat brain. II mesencephalon, rhombencephalon, and spinal cord. Exp Brain Res 78:164–173
Harting JK, Updyke BV, Van Lieshout DP (1992) Cortico-tectal projections in the cat: anterograde transport studies on twenty-five cortical areas. J Comp Neurol 324:379–414
Harvey AR, Worthington DR (1990) The projection from different visual cortical areas to the rat superior colliculus. J Comp Neurol 298:281–292
Hilbig H (1991) Zur Struktur des Collculus superior beim Mikrophthalmusmäusestamm 944. J Hirnforsch 32:135–138
Hilbig H (1996) Morphometric analysis of neurons in the superficial layers of rat superior colliculus. In: Elsner N, Schnitzler HU (eds) Brain and evolution. Thieme, Stuttgart New York, p 89
Hilbig H, Schierwagen A (1994) Interlayer neurons in the rat superior colliculus: a tracer study using DiI/Di-ASP. Neuroreport 5:477–480
Hilbig H, Winkelmann E (1993) NADPH-diaphorase staining of the superior colliculus of the rat – distribution and morphology. Verh Anat Ges 88:215
Huerta MF, Harting JK (1984) Connectional organization of the superior colliculus. Trends Neurosci 7:286–289
Hunt SP Künzle H (1976) Observations on the projections – an autoradiographic study based on anterograde and retrograde axonal and dendritic flow. J Comp Neurol 170:153–163
Illing RB (1988) Spatial relation of the β-acetylcholinesterase-rich domain to the visual topography in the feline superior colliculus. Exp Brain Res 73:589–594
Illing RB (1989) The mosaic of the retinal projection in the superior colliculus of the cat. Exp Brain Res 74:641–644
Illing RB, Graybiel A (1993) Pattern formation in the developing superior colliculus: ontogeny of the periodic architecture in the intermediate layers. J Comp Neurol 339:1–17
Illing RB, Vogt DM, Spatz WB (1990) Parvalbumin in rat superior colliculus. Neurosci Lett 120:197–200
Jeon C, Mize RR (1993) Choline acetyltransferase-immunoreactive patches overlap specific efferent cell groups in the cat superior colliculus. J Comp Neurol 337:127–150
Kosaka T, Heizmann CW (1989) Selective staining of a population of parvalbumin-containing GABAergic neurons in the rat cerebral cortex by lectins with specific affinity for terminal N-acetylgalactosamine. Brain Res 483:158–163
Labriola AA, Laemle LK (1977) Cellular morphology in the visual layer of the developing rat superior colliculus. Exp Neurol 55:247–268
Laemle LK (1981) A Golgi study of cellular morphology in the superficial layers of superior colliculus of man, *Saimiri*, and *Macaca*. J Hirnforsch 22:253–263
Laemle LK (1983) A Golgi study of cell morphology in the deep layers of the human superior colliculus. J Hirnforsch 24:297–306
Lander C, Zhang H, Hockfield S (1998) Neurons produce a neuronal cell surface-associated chrondroitin sulfate proteoglycan. J Neurosci 18:174–183
Langer TP, Lund RD (1974) The upper layers of the superior colliculus of the rat: A Golgi study. J Comp Neurol 158:405–436
Legrande A, Alonso G (1998) Pregnenolone reverses the age-dependent accumulation of glial fibrillary acidic protein within astrocytes of specific regions of the rat brain. Brain Res 802:125–133
Leuba G, Saini K (1996) Calcium-binding proteins immunoreactivity in the human subcortical and cortical visual structures. Vis Neurosci 13:997–1009
Levitt P, Rakic P (1980) Immunoperoxidase localization of radial glial fibrillary acidic protein in radial glial cells and astrocytes of the developing rhesus monkey brain. J Comp Neurol 193:815–840
Lindsay RM (1986) Reactive gliosis in astrocytes. In: Fedoroff S, Vernadakis A (eds) Cell biology and pathology of astrocytes. Academic Press, Oxford, pp 231–262
Mize RR (1992) The organization of GABAergic neurons in the mammalian superior colliculus. Prog Brain Res 90:219–248
Mize RR, Jeon CJ, Butler GD, Luo Q, Emson PC (1991) The calcium-binding protein calbindin-D 28 K reveals subpopulations of projection and interneurons in the cat superior colliculus. J Comp Neurol 307:417–436
Mooney RD, Klein BG, Rhoades RW (1985) Correlations between the structural and functional characteristics of neurons in the superficial laminae of the hamsters superior colliculus. J Neurosci 5:2989–3009
Naegele JR, Katz LC (1990) Cell surface molecules containing N-acetylgalactosamine are associated with basket cells and neuroglioform cells in cat visual cortex. J Neurosci 10:540–557
Oermann EA (1996) Nachweis von NO-Synthasen während der Ontogenese im Säugerhirn. Diploma Thesis, Faculty of Biology, University of Düsseldorf, pp 1–110
Pappas CA, Ransom B (1994) Depolarization-induced alkalinization (DIA) in rat hippocampal astrocytes. J Neurophysiol 72:2816–2826
Pellerin L, Magistretti PJ (1994) Glutamate uptake into astrocytes stimulates aerobic glycolysis: a mechanism coupling neuronal activity to glucosutilization. Proc Natl Acad Sci USA 91:10625–10629

Publido-Caballero J, Jimenez-Sampedro F, Echevarria-Aza D, Martinez-Millan L (1994) Postnatal development of vimentin-positive cells in the rabbit superior colliculus. J Comp Neurol 343:102–112

Reese B (1984) The projection from the superior colliculus to the dorsal lateral geniculate nucleus in the rat. Brain Res 305:162–168

Robello M, Baldelli P, Cupello A (1994) Modulation by extracellular pH of the activity of GABA receptors on rat cerebellum granule cells. Neurscience 61:833–837

Robinson DL, McClurkin JW (1989) The visual superior colliculus and pulvinar. In: Wurtz RH, Goldberg W (eds) The neurobiology of saccadic eye movements. Elsevier, Amsterdam, pp 337–340

Romeis B (1989) Mikroskopische Technik. Urban & Schwarzenberg, München Wien Baltimore

Sahibzada N, Yamasaki D, Rhoades RW (1987) The spinal and commissural projections from the superior colliculus in rat and hamster arise from distinct neuronal populations. Brain Res 415:242–256

Schmidt-Kastner R, Wietasch K, Weigel H, Eysel UT (1993) Immunohistochemical staining for glial fibrillary acidic protein (GFAP) after deafferentation or ischemic infarction in rat visual system: Features of reactive and damaged astrocytes. Int J Dev Neurosci 11:157–174

Seeger G, Brauer K, Härtig W, Brückner G (1994) Mapping of perineuronal nets in the rat brain stained by colloidal iron hydroxide histochemistry and lectin cytochemistry. Neuroscience 58:371–388

Seeger G, Lüth H J, Winkelmann E, Brauer K (1996) Distribution patterns of *Wisteria floribunda* agglutinin binding sites and parvalbumin-immunoreactive neurons in the human visual cortex: a double-labelling study. J Hirnforsch 36:351–366

Sugita S, Otani K, Tokunaga A, Terasawa K (1983) Laminar origin of the tecto-thalamic projections in the albino rat. Neurosci Lett 43:143–147

Tokunaga A (1970) Neuronal structure of the superior colliculus of the rat. J Chiba Med Soc 46:289–299

Tokunaga A, Otani K (1976) Dendritic pattern of neurons in the rat superior colliculus. Exp Neurol 52:189–205

Valverde F (1973) The neuropil of the superficial layers of the superior colliculus of the mouse. A correlated Golgi and electronmicroscopic study. Z Anat Entwicklungsgesch 142:117–147

Vanegas H (1984) Comparative neurology of the optic tectum. Plenum Press, New York London

Wallace MN (1986a) Spatial relationship of NADPH-diaphorase and acetylcholinesterase lattice in rat and mouse superior colliculus. Neuroscience 19:381–391

Wallace MN (1986b) Spatial relationship of histochemically demonstrable patches in the mouse superior colliculus. Exp Brain Res 62:241–249

Werner L, Krüger G (1973) Qualitative und quantitative Untersuchungen am Corpus geniculatum laterale (CGL) der Laborratte. III. Differenzierung von Projektions und Interneuronen im Nissl-Präparat und deren Topographie. Z Mikrosk Anat Forsch 87:701–729

Werner L, Wilke A, Bloedner R, Winkelmann E, Brauer K (1982) Topographical distribution of neuronal types in the albino rat's area 17. A qualitative and quantitative Nissl study. Z Mikrosk Anat Forsch 96:433–453

Wurtz RH (1996) Vision for the control of movement. Invest Ophthalmol Vis Sci 37:2131–2145

Yamasaki DS, Krauthammer G, Rhoades RW (1984) Organization of the intercollicular pathway in rat. Brain Res 300:368–371

Zilles K, Hajos F, Kalman M, Schleicher A (1991) Mapping of glial fibrillary acidic protein immunoreactivity in the rat forebrain and mesencephalon by computerized image analysis. J Comp Neurol 308:340–355